Journal of Medicinal and Nanomaterials Chemistry, 2019, 1(1), 99-110.

FULL PAPER

Vitex negundo leaf extract mediated synthesis of ZnO nanoplates and its antibacterial and photocatalytic activities

M. Anbuvannan[a,*], M. Ramesh[b], E. Manikandan[c], R.Srinivasan[d]

[a] *Department of Physics, Sri Akilandeswari Women's College, Wandiwash-604408, Tamil Nadu, India.*
[b]*Department of Physics, M.V. Muthiah Government Arts College for Women, Dindigul- 624 001,Tamil Nadu, India.*
[c]*Department of Physics ,Thiruvalluvar University College of Arts & Science, Thennangur-604408, Tamil Nadu, India.*
[d] *Tamil Nadu State Council for Science and Technology (TNSCST), DOTE Campus, Chennai-600 025, Tamil Nadu, India.*

Received: 11 September 2018, Revised: 24 November 2018 and Accepted: 30 December 2018.

ABSTRACT: The ZnO nanocrystals were prepared using *vitex negundo* leaf extract via a simple green method. The confirmation of ZnO formation was carried out by UV–Vis-diffuse reflectance spectroscopy (UV-Vis DRS). The prepared nanocrystals were further characterized by photoluminescence (PL), X-ray diffraction (XRD), Fourier transform infrared spectroscopy (FT-IR), field emission-scanning electron microscopy (FE-SEM) and transmission electron microscopy (TEM). The FE-SEM results confirmed that the ZnO nanoparticles were nanosize. To assess the photocatalytic activities of ZnO nanocrystals, the degradation of methylene blue (MB) under UV radiation was analyzed. In addition, the antibacterial activities of synthesized ZnO nanoparticles were screened against the *S. aureus*, *S. paratyphi*, *V. cholerae*, and *E. coli*.

KEYWORDS: Zinc oxide, *Vitex negundo*, Nanoplate, Photocatalytic, Antibacterial activity.

GRAPHICAL ABSTRACT:

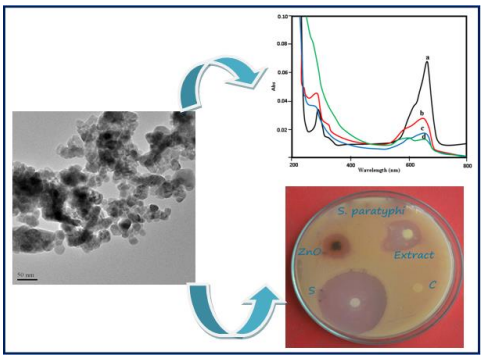

1. Introduction

Over the last few years, the micro and nanostructured ZnO material has consumed ample space due to their wide range of applications. Zinc oxide is an II–VI semiconductor with a band gap of 3.37 eV; it is thermally and chemically stable [1]. Also, ZnO is a more multifunctional material with wide applications due to its excellent chemical and thermal stability, wonderful optical and electrical properties [2]. It has been extensively studied and applied in transistors [3], solar cells [4], piezoelectric transducers [5], gas sensors [6], and photo catalysts [7]. Recently, there has been report regarding the antimicrobial activity of ZnO nanoparticles [8]. Most of the properties of the ZnO strongly depend on its structures, including the morphology, size and aspect ratio [9]. Nowadays, control

*Corresponding author: M. Anbuvannan, E-mail: anbuphy85@gmail.com , Tel: 91- 9843318360

of the morphology and size of particulate inorganic materials has received increased great attention. Therefore, it is important to develop facile method to prepare high quality ZnO with uniform morphologies. There are several physical and chemical procedures have been used for the synthesis of large quantities of metal nanoparticles in relatively short period of time. ZnO nanostructures could be synthesized via physical methods such as molecular beam epitaxy (MBE) [10], physical vapor deposition (PVD) [11], laser deposition [12], and also chemical methods including chemical bath deposition (CBD) [13], hydro-thermal synthesis [14], and sol–gel process [15-17], respectively. Recently, plant-mediated biological synthesis of nanoparticles has attracted a great deal of attention due to its simplicity, eco-friendliness, and extensive catalytic and antimicrobial activity.

2. Materials and Methods

2.1. Preparation of Leaf Extract

Vitex negundo plant leaves were collected from Polur, Thiruvannamalai District (12°15' N, 79°07' E), Tamil Nadu, India. The collected leaves washed several times with distilled water to remove the dust particles. In the preparation of the leaves extract, 20 g of fine cut leaves in 250 mL glass beaker mixed with 100 mL of distilled water. Boiling of the mixture for 20 min changed the color of the aqueous solution from watery to light yellow. After allowing the extract to cool to room temperature, using a Whatman filter paper broth filtration took place.

2.2. Preparation of ZnO NPs

To synthesize the ZnO nanoparticles, 30, 40, and 50 mL of *Vitex negundo* leaves extract boiled using a stirrer–heater. Then, 5 gm of zinc nitrate added to the above solution as the temperature reached 60 °C. The mixture further boiled until the color changed into a dark yellow. The obtained paste transformed to the ceramic crucible and annealed at 400 °C for 2 h. The finally arrived light white colored powder consumed for different characterizations.

2.3. Characterization of ZnO NPs

The UV–Vis reflectance spectra (UV–Vis DRS) measurements were carried out using a UV140404B with the wavelength of 200-850 nm at the reflectance mode. The photoluminescence (PL) spectra were recorded using FLUOROLOG - FL3-11 fluorescence spectrometer. The crystalline structure of the samples was analyzed using a X-Ray diffractometer (PAN analytical X'PERT PRO model), operating at the voltage of 50 kV and current of 30 mA. Fourier transform infrared spectra were recorded under identical conditions in the 4000-400 cm^{-1} region using Fourier transform infrared spectrometer (SHIMADZHU). The morphology and size distribution were characterized using FE-SEM (JEOL JSM 6701-F) and TEM in a JEM–2100, 200KV, JEOL available at SAIF, Shillong, respectively.

2.4. Photocatalytic Activity Measurement

Photocatalytic activities of the ZnO nanoparticles were determined by the photodegradation of Methylene Blue (MB) in aqueous solution under the UV radiation. Heber Multilamp photoreactor (HML MP 88) was used to study the degradation by UV-A light (365 nm) [18]. The

Journal of Medicinal and Nanomaterials Chemistry

reduction of the MB was taken place due to the catalytic activity of the as prepared metal nanoparticles. The dye of MB (1×10^{-4} M) with the appropriate amount of catalyst (20 mg) was stirred for 30 min in the dark prior to illumination to achieve maximum adsorption of MB onto the semiconductor surface. The progress of the reaction was subsequently followed at different time intervals using UV–Visible spectrophotometer. The entire reduction reaction experiment was conducted under UV irradiation. The intensity of the blue color of the reaction mixture decreased gradually, and eventually turned colorless. The absorbance for MB at 665 nm, monitored with UV–Vis spectrometer, was an indication of catalytic activity of ZnO particles.

2.5. Antimicrobial Assay

The synthesized compound tested for inhibition against the human pathogenic bacteria. Microbial assay was conducted using the Kelmanl disc diffusion method [19]. The pathogens namely *Salmonella paratyphi*, *Vibrio cholerae*, *Staphylococcus aureus* and *Escherichia coli*, were obtained from Raja Sir Muthaiya Medical College, Annamalai University. 150 CFU/mL of inoculums was swabbed onto MH-agar plates uniformly and allowed to dry in a sterile environment. Sterile disc of 6 mm (HIMEDIA) were loaded with 20 µL of test solution (solvent, leaf extract, and ZnO NPs). Ampicillin (10 mg in 1 mL) was used as positive control. The plates were incubated at 25 °C for 3 days to measure zone of inhibition. Mean was calculated by performing the experiments in triplicates.

3. Results and Discussion

3.1 Optical Studies

Fig.1 shows the optical absorption spectrum of ZnO NPs synthesized using *Vitex negundo* extract. The sample had a clear and strongly observed absorption peak below at 400 nm. The band gap energy (E_g) of ZnO was obtained from the wavelength value corresponding to the intersection point of the vertical and horizontal part of the spectrum, using the equation 1.

$$E_g = \frac{hc}{\lambda} eV \; ; \; E_g = \frac{1240}{\lambda} eV \qquad (1)$$

Where, Eg is the band gap energy (eV), h is the Planck's constant (6.626 x 10-34 Js), C is the light velocity (3 x108 m/s) and λ is the wavelength (nm). The band gap energy corresponds to the absorption limit and can be roughly evaluated by the above relation. From Fig. 1, the absorption edges are positioned at 365, 360 and 355 nm, which corresponding to the band gap value of 3.39, 3.44 and 3.49 eV. The blue shift of absorption maximum indicates the quantum confinement effect.

3.1b Indirect Band Gap Energy (Kubelka–Munk Plot)

The reflectance spectra were analyzed using the Kubelka- Munk relation (Equation 9). To convert the reflectance data into a Kubelka-Munk function (equivalent to the absorption coefficient) F (R), the following relation was used.

$$F(R) = \frac{(1-R)^2}{2R} \qquad (2)$$

where, R is the reflectance value. Band gap energy of the sample was estimated from the variation of the Kubelka-Munk function with photon energy. Fig.2. demonstrates the Kubelka-Munk plots for the ZnO NPs. It is

used to determine the band gap energy associated with their indirect transitions. The ZnO exhibits indirect band gap of 3.40, 3.44 and 3.47 eV, respectively for 30, 40, and 50 mL of extract addition.

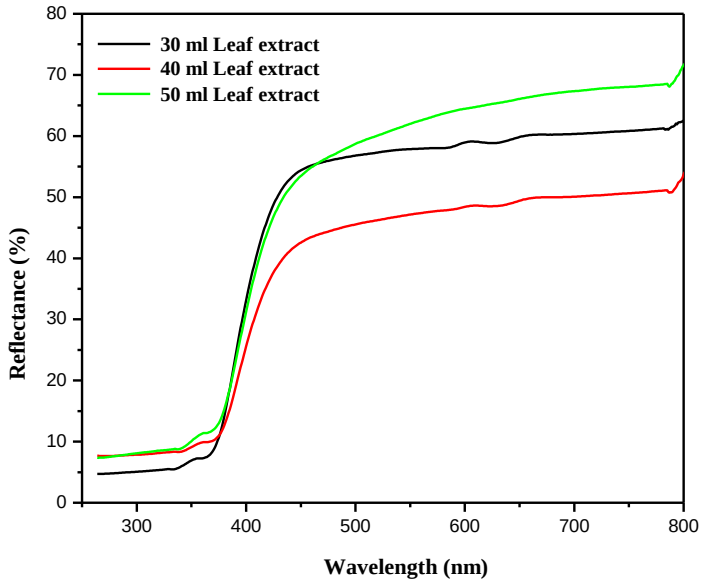

Fig.1. UV-DRS spectrum of ZnO NPs synthesized using different proportions of *Vitex negundo* leaf extract

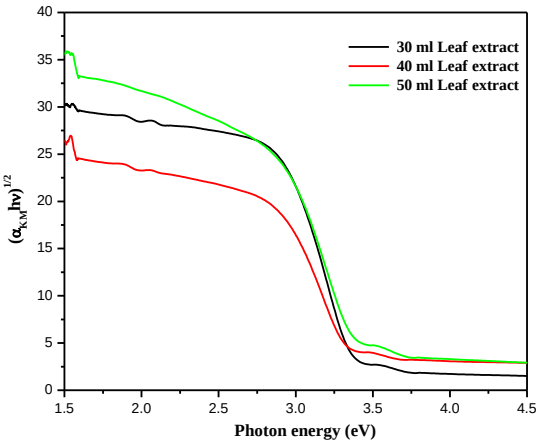

Fig. 2. Plot of indirect band gap energy for ZnO NPs

3.2 Photoluminescence Spectroscopy

PL measurement is an efficient way to estimate the defects and optical properties of the prepared samples. Fig. 3 exhibits the PL emission properties of the ZnO prepared from different levels of extract addition. As shown in the Fig. 3, all the samples have high UV emission at 402 nm. The intense UV emission is the near band edge emission of ZnO originating from the recombination of excitons [20]. In addition, the ZnO derived from 30 and 40 mL of extract addition shows faintly visible emissions at 432 and 443 nm. The faint visible emissions at 432 and 447 nm probably originated from oxygen vacancies or other detects [21]. However, on 50 mL of extract addition, the visible emissions (432, and 447 nm) showed a red-shift (471 and 483 nm) with the creation of a new visible radiation at 530

nm. The origin of green emission at 530 nm ascribed from the single – ionized oxygen vacancies [22–24]. From PL results, it is evident that 50 mL of extract addition creates more oxygen vacancies.

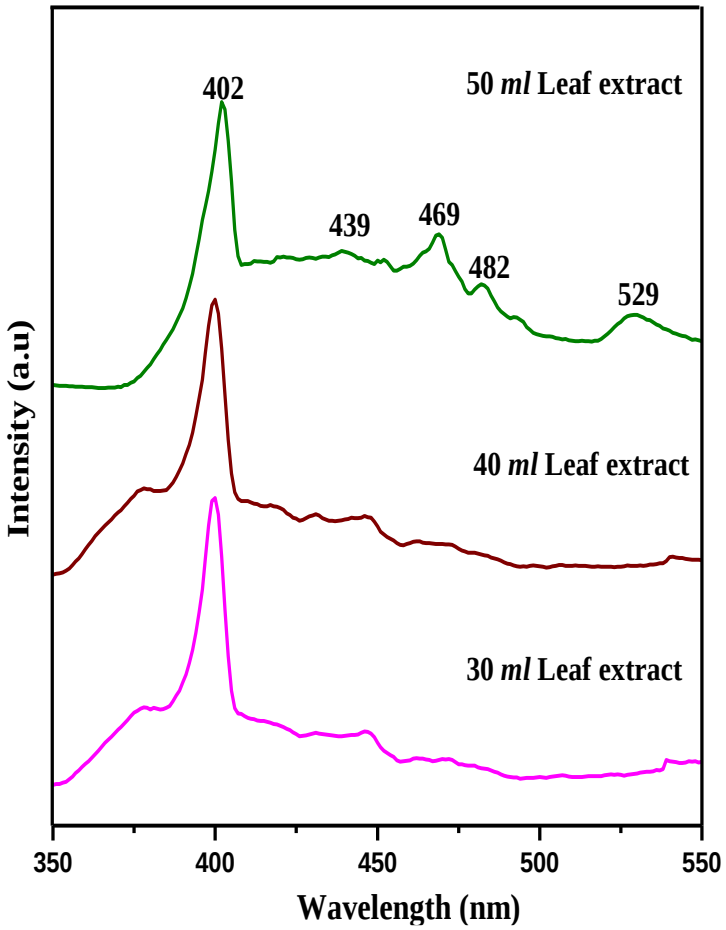

Fig.3. Photoluminescence spectrum of ZnO NPs synthesized using different proportions of *Vitex negundo* leaf extract.

3.3 Structure Analysis

Fig. 4 illustrates the diffraction results of ZnO prepared from different levels of extract addition. All the samples show diffractions from (100), (002), (101), (102), (110), (103), (201), (112), (201), and (202) plane of reflections indicating the single phase wurzite structure of ZnO [25] as specified in the standard card. (JCPDS No. 89-1397). The average crystalline size of the synthesized ZnO nanoparticles were calculated using the Scherrer's equation and found to be 39.87, 33.68 and 23.81 nm, respectively for 30, 40, and 50 mL of extract addition.

$$D = \frac{K\lambda}{\beta \cos\theta} \text{Å} \quad (3)$$

where D is particle diameter, K is a constant equal 0.9, λ is wavelength of X-ray source (λ=1.5406Å), β is the full width at half maximum (FWHM) and θ is the diffraction angle, respectively.

3.4 FTIR Analysis of ZnO-NPs

FTIR absorption spectra of the biosynthesized ZnO-NPs are shown in the Fig. 5. The band of biosynthesized *ZnO-NPs* from *Vitex negundo* were observed at 2924, 2353, 1633, 1440, 1382, 1026, 848,

Journal of Medicinal and Nanomaterials Chemistry

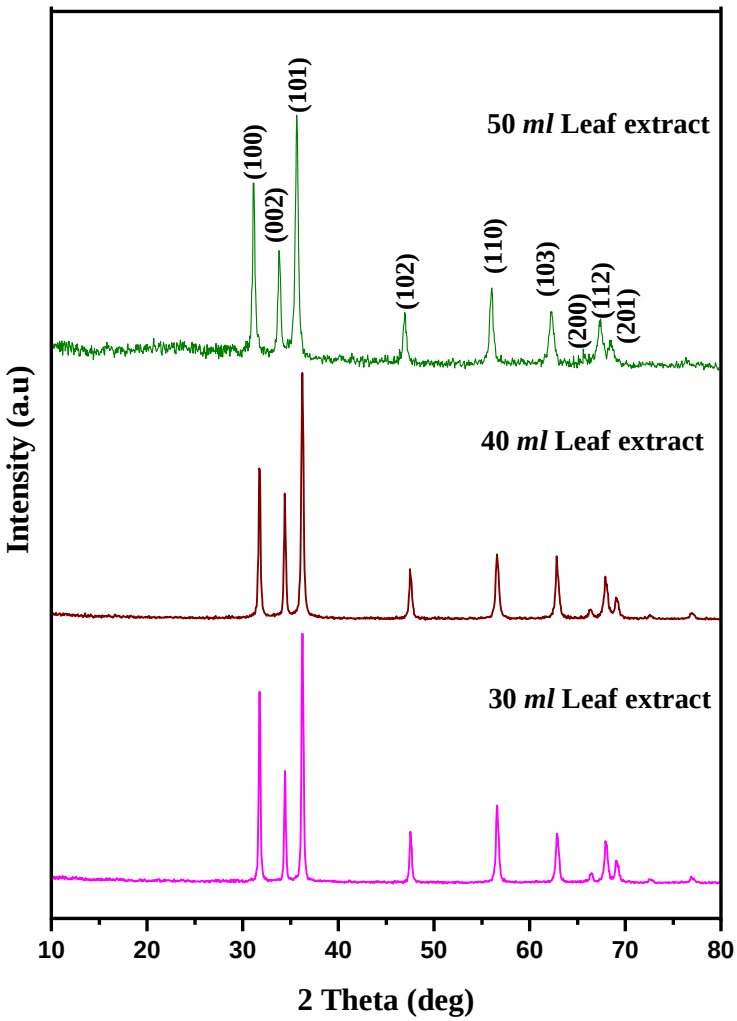

Fig.4. XRD spectrum of ZnO NPs synthesized using different proportions of *Vitex negundo* leaf extract.

and 437 cm^{-1}, respectively in the FTIR spectrum, whereas, the bands of *Vitex negundo* extract were noticed at 3426, 2924, 1643, 1264, 1041, and 621 cm^{-1}, respectively. The broad and intense band at 3237-3565 cm^{-1} is due to O-H stretching [26]. The intense broad band at 3426, 2353 cm^{-1} can be assigned as O-H and C=O stretching vibration. The absorption band corresponding to 3426 cm^{-1} was due to the C-H stretching vibrations of carboxylic acid and hydroxyl stretch vibrations. FTIR spectrum of ZnO-NPs showed absorption band at 1633 cm^{-1}, corresponding to the amide I of polypeptides [27]. The bands ~ 1440 cm^{-1} are attributed to the C-H bending. The peak at around 1264 cm^{-1} present in both the samples, it signified as amide III band of the random coil of protein [28]. The peaks at 2924 cm^{-1} might show the C-H Stretch. The band at 1026 cm^{-1}, which are sharper and broader for ZnO nanoparticles, participates in the reaction [29]. The band 849 cm^{-1} can be assigned as aromatic C-H out of plane bending.

Journal of Medicinal and Nanomaterials Chemistry

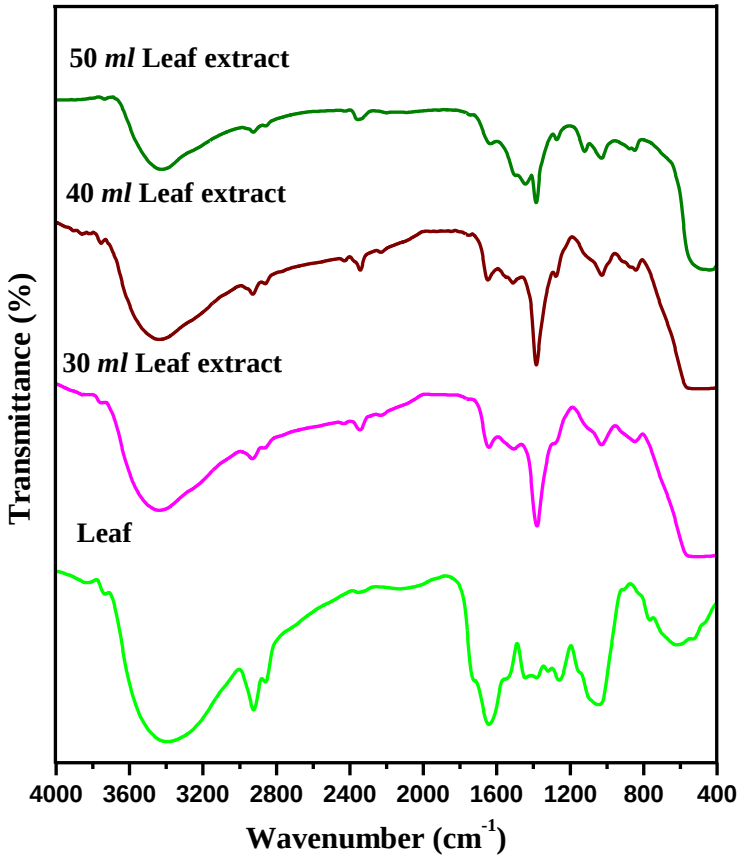

Fig.5. FT-IR spectra of leaf and ZnO NPs synthesized using different proportions of *Vitex negundo* leaf extract.

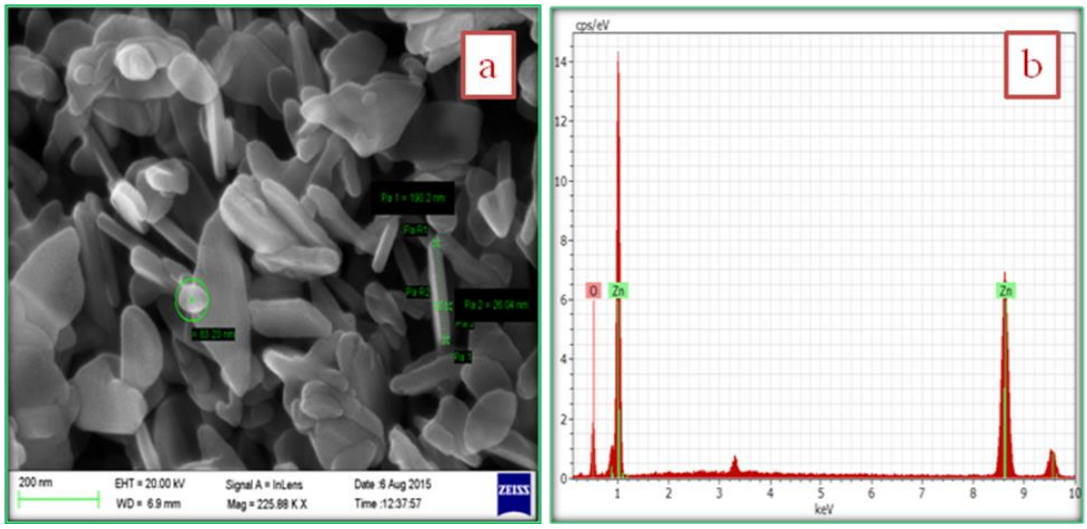

Fig.6. a) FE–SEM image and **b)** EDX spectrum of ZnO NPs synthesized using 50 ml of *Vitex negundo* leaf extract**.**

3.6 TEM Analysis

The morphology and microstructure of the nanoparticles were further characterized using TEM analysis. Figure 7-a reveals that the most of the ZnO nanoparticles were quasi-spherical with the size of 23.81 nm. The selected area electron diffraction indicates the nanoparticles are polycrystalline in nature as shown in Figure

7-b. The particle size determined by the TEM analysis is in good agreement with that of the XRD analysis.

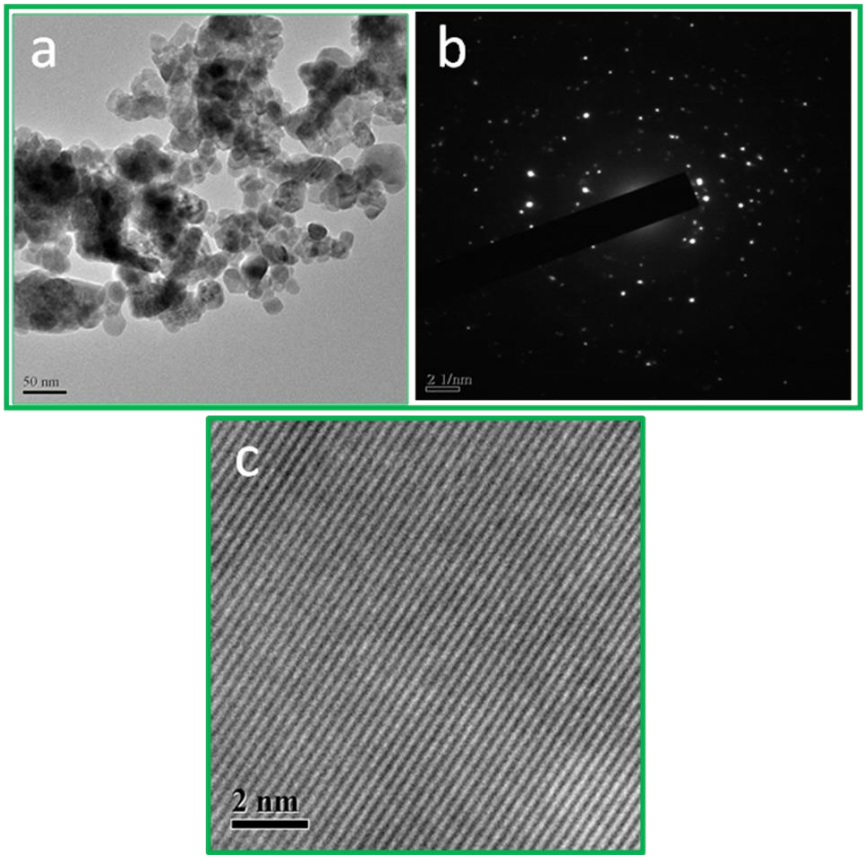

Fig.7. TEM image ZnO nanostructures (a), SAED patterns (b),Corresponding HRTEM image (c).

3.7 Photocatalytic activity

To demonstrate the potential environmental application in the removal of contaminants from wastewater, the photocatalytic activities of the as-synthesized ZnO nanoparticles were investigated by degradation of MB. The catalytic testing of MB in our work is performed as follows: for comparison, a blank test is conducted with a mixture of MB dye. Within 30 min, there is no decrease of absorbance of MB at 665 nm monitored by UV (Figure 8a), indicating that the catalytic reduction of MB did not occur. And the color of the solution was not changed, at all with time gone. However, when the experiment was carried out by ZnO nanoparticles was introduced; the color of the solution is changed significantly from blue to colorless. The track of ultraviolet–visible (UV–Vis) spectroscopy is shown in Figure 8(b-d). As can be seen, the absorbance at 665nm of MB gradually decreases after 30 min along with the process of reduction reaction, which indicates that the catalytic reduction of MB has proceeded successfully.

The plausible mechanism for the photocatalytic degradation of the MB dye can be schematically shown as following.

$$\text{Photocatalysts (ZnO)} + h\nu \rightarrow e^{-} + h^{+} \quad (1)$$

$$h^{+} + H_2O \rightarrow H^{+} + OH^{\bullet} \quad (2)$$

$$h^{+} + OH^{-} \rightarrow OH^{\bullet} \quad (3)$$

$$e^{-} + O_2 \rightarrow O_2^{-} \quad (4)$$

$$2e^{-} + O_2 + 2H^{+} \rightarrow H_2O_2 \quad (5)$$

$$e^{-} + H_2O_2 \rightarrow OH^{\bullet} + OH^{-} \quad (6)$$

Organic + $^{\bullet}OH$ + O_2 → CO_2 + H_2O + other degradation productions (7)

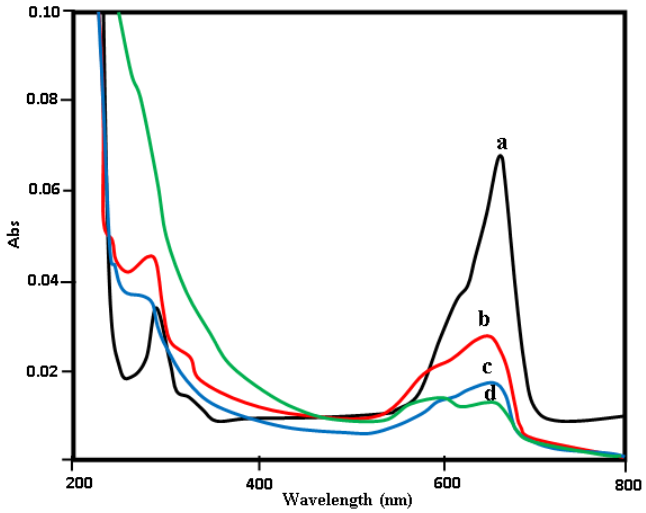

Fig.8. UV–Visible spectra of methylene blue reduction by 50 ml of *Vitex negundo* leaf extract presence of ZnO NPs.

The excited dye injects an electron to the conduction band of ZnO, and scavenged by pre-adsorbed oxygen, O_2, to form active oxygen radicals. These generated active radicals that drove the photodegradation process. The as-prepared ZnO nanoparticles play an important role as an electron carrier. Such assisted photo processes provide an attractive path for the treatment of dye (Figure 9).

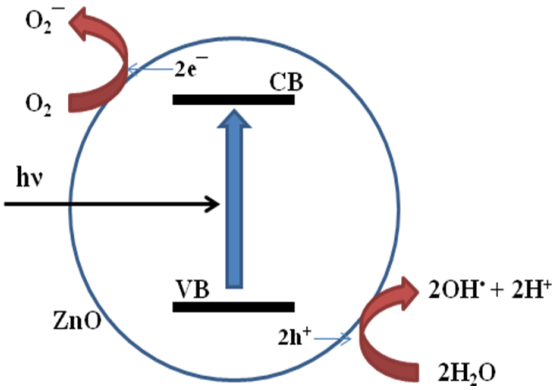

Fig.9. Schematic of the photocatalytic mechanism for ZnO photocatalysts

3.8 Antibacterial Activity of ZnO-NPs

Antimicrobial activities of the metal oxide (ZnO, MgO, and CaO) powders against the *Staphylococcus aureus*, *Escherichia coli*, or fungi were quantitatively evaluated in culture media [30, 31]. Antibacterial activity of the green synthesized ZnO nanoparticles towards various human pathogens was tested by disc diffusion methods, represented in the Figure 9. ZnO nanoparticles showed antimicrobial activity against the selected pathogens but maximum activity was observed in *V. cholerae* (21 mm), *S. paratyphi* (7 mm) (Figure 9 a, c). In the present study, green ZnO nanoparticles showed a greater significant zone inhibition when compared to leaf extract and standard tablet. Lower activity was observed in *S. aureus* (8 mm), *E. coli* (2 mm) when compared to standard tablet. Both extract and ZnO nanoparticles showed antimicrobial activity against

selected pathogens but no activity was observed for control distilled water. Previously, the biological synthesized ZnO nanoparticles using aloe leaf broth also showed a similar potent bactericidal activity [32].

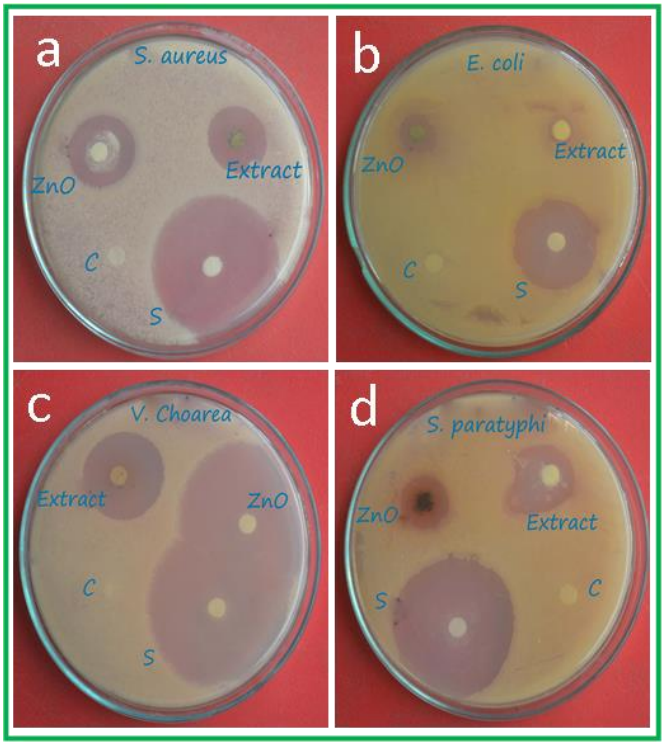

Fig.10. Antibacterial activity of ZnO NPs synthesized using 50 ml of Vitex negundo leaf extract.

Conclusion

We have successfully used a plant material for the consistent and quick synthesis of ZnO nanoparticles. Synthesis of the ZnO-NPs using green resource *Vitex negundo* has a better alternative to chemical synthesis, since this green synthesis is pollutant free and eco-friendly. UV-Vis-DRS reveled the corresponding the band gap value of ZnO-NPs was 3.41 eV, which indicates red shift in the UV region. PL spectrum of the ZnO NPs was measured at the wavelength of 350 nm. The FE-SEM results revealed the plate-like nanostructures of the ZnO particles. The particle size of 23.83 nm determined from TEM analysis was in good agreement with that of the XRD. In addition, the photocatalytic performance of the ZnO tested against the methylene blue (MB) dye under UV radiation had a significant photodegradation. Antibacterial activities of the prepared products analyzed against some selected human pathogens showed excellent results.

Acknowledgments

The authors are thankful and grateful to Department of Physics, Annamalai University, Tamilnadu–608 002 and Sri Akilandeswari Women's College, Wandiwash, Tamil Nadu, India – 604 408 for providing all necessary facilities to carry out the present work successfully.

Reference

1. Z. Gao, Y. Gu, Y. Zhang, (**2010**) *J. Nanomater.*, **10**: 1-5
2. S. Cho, J. Jang, S. Jung, B.R. Lee, E. Oh, K. Lee, (**2009**) *Langmuir.*, **25**: 3825–3831.

3. B.S. Ong, C.S. Li, Y.N. Li, Y.L. Wu, R. Loutfy, (**2007**) *J. Am. Chem. Soc*., **129**:2750–2751.
4. J.J. Wu, Y.R. Chen, W.P. Liao, C.T. Wu, C.Y. Chen, (2010) *ACS Nano*., **4**:5679–5684.
5. D. Choi, M.Y. Choi, W.M. Choi, H.J. Shin, H.K. Park, J.S. Seo, J. Park, S.M. Yoon, S.J. Chae, Y.H. Lee, S.W. Kim, J.Y. Choi, S.Y. Lee, J.M. Kim, (**2010**) *Adv. Mat.*, **22**:2187–2192.
6. M.J.S. Spencer, I. Yarovsky, (**2010**) *J. Phys. Chem.* C., **114**:10881–10893.
7. Z. Han, L. Liao, Y. Wu, H. Pan, S. Shen, J. Chen, (**2012**) *J. Hazard. Mat.*, **217**:100–106.
8. A. Yadav, V. Prasad, A.A. Kathe, S. Raj, D. Yadav, C. Sundarmoorthy, N. Vigneshvaran, (**2006**) *Bull. Mater. Sci.*, **29**: 641-645.
9. C. Lui, Y. Masuda, Y. Wu, O. Takai, (**2006**) *Thin Sol. Films*, **503**:110–114.
10. D.C. Look, D.C. Reynolds, C.W. Litton, (**2002**) *Appl. Phys. Lett.*, **81**: 1830–1832.
11. Y.C. Kong, D.P. Yu, B. Zhang, (2001)*Appl. Phys. Lett.*,**78**: 407–409.
12. B.J. Jin, S. Im, S.Y. Lee, (**2002**) *Thin Sol. Films.*, **366** :107–110.
13. V.R. Shinde, C.D. Lokhande, S.H. Han, (**2005**) *Appl. Surf. Sci.*, **245**:407–413.
14. B. Liu, H.C. Zeng, (**2003**) *J. Am. Chem. Soc.*, **125**: 4430–4431.
15. Y. Ohya, T. Ogata, Y. Takahashi, (2005) *J. Ceram. Soc. Jpn*., **113**:220–225.
16. L. Znaidi, C. Sanchez, A.V. Kanaev, (**2003**) *Thin Sol.Films.*, **428**:257–262.
17. M.S. Tokumoto, S.H. Pulcinelli, V. Briois, (**2003**) *J. Phys. Chem. B.*, **107** :568–574.
18. A. Senthilraja, B. Subash, B. Krishnakumar, D. Rajamanickam, M. Swaminathan, M. Shanthi, (**2014**) *Mat. Sci. Semiconductor Proc.*, **22**: 83–91.
19. D. Kelman, Y. Kashman, E. Rosenberg, M. Ilan, I. Iirach, Y. Loya, (**2001**) *Aquat. Microb. Ecol.*,**24**:9–16.
20. K.V. Vanheusden, W.L. Warren, C.H. Seager, (**1996**) *J. Appl. Phys.*, **79**:7983-7990.
21. M. Anbuvannan, M. Ramesh, G. Viruthagiri, N. Shanmugam, (**2015**) *Mater Sci Semicond Process.*, **39** :621–628.
22. Y. W. Heo, D. P. Norton, S. J. Pearton, (**2005**) *J. Appl. Phys.*, **98**: 073502.
23. B. Lin, Z. Fu, Y. Jia, (**2001**) *Appl. Phys. Lett.*, **79**: (7) 943.
24. M.H. Huang, Y. Wu, H. Feick, N. Tran, E. Weber, P. Yang, (2001) *Adv. Mater*,. **13**: 113.
25. S. Mridha, D. Basak, (2007) *Mater. Res. Bull.* 42:875–882.
26. D. Gnanasangeetha, D. Sarala Thambavani, (2013) *Res. J. Mat. Sci.* 1:1–8.
27. R. Sathyavathi, M.B. Krishna, S.V. Rao, R. Saritha, D.N. Rao, (2010) *Adv Sci Lett* 3:1–6.
28. S. Cai, B.R. Singh, (2004) *Biochem.* 43: 2541–2549.

29. S. Nagarajan K. Arumugam Kuppusamy,(2013) *J.of Nanobiotech*,11:39.
30. J. Sawai, (2003) *J. Micro. Meth.* 54 :177–182.
31. J. Sawai, T. Yoshikawa, (2004) *J. App. Micro.* 96 :803–809.
32. S. Gunalana, R. Sivaraja, V. Rajendran, (2012) *Prog. Nat. Sci. Mat. Inter.* 22:693–700.

How to cite this manuscript: M. Anbuvannan*, M. Ramesh, E. Manikandan, R.Srinivasan. Vitex negundo leaf extract mediated synthesis of ZnO nanoplates and its antibacterial and photocatalytic activities. Journal of Medicinal and Nanomaterials Chemistry, 2019, **1**(1) , 99-110.